



HAL
open science

Morphological analysis of tumor cell/endothelial cell interactions under shear flow.

Roxana Chotard-Ghodsnia, Oualid Haddad, Anne Leyrat, Agnès Drochon,
Claude Verdier, Alain Duperray

► **To cite this version:**

Roxana Chotard-Ghodsnia, Oualid Haddad, Anne Leyrat, Agnès Drochon, Claude Verdier, et al.. Morphological analysis of tumor cell/endothelial cell interactions under shear flow.. *Journal of Biomechanics*, 2007, 40 (2), pp.335-44. 10.1016/j.jbiomech.2006.01.001 . inserm-00144469

HAL Id: inserm-00144469

<https://inserm.hal.science/inserm-00144469>

Submitted on 4 May 2007

HAL is a multi-disciplinary open access archive for the deposit and dissemination of scientific research documents, whether they are published or not. The documents may come from teaching and research institutions in France or abroad, or from public or private research centers.

L'archive ouverte pluridisciplinaire **HAL**, est destinée au dépôt et à la diffusion de documents scientifiques de niveau recherche, publiés ou non, émanant des établissements d'enseignement et de recherche français ou étrangers, des laboratoires publics ou privés.

Morphological analysis of tumor cell/ endothelial cell interactions under shear flow**Roxana Chotard-Ghodsni^{1*}, Oualid Haddad^{2,3}, Anne Leyrat¹, Agnès Drochon⁴, Claude Verdier¹, Alain Duperray^{2,3}**¹ Laboratoire de Spectrométrie Physique, UMR 5588 (CNRS- Université Grenoble I)

BP 87, 140 Rue de la Physique, 38402 Saint-Martin d'Hères, France;

² INSERM, U578, Grenoble, France;³ Université Grenoble I, Groupe de Recherche sur le Cancer du Poumon, Institut Albert Bonniot, Grenoble, France;⁴ Biomécanique et Génie Biomédical, UMR 6600 (CNRS- Université de Technologie de Compiègne), BP 20529, 60205 Compiègne Cedex, France**Word count (introduction through discussion): 3760****Keywords:** metastasis, extravasation, endothelium, flow, cancer

* Corresponding author: Laboratoire de Spectrométrie Physique (UMR5588)

BP 87, 140 Rue de la Physique, 38402 Saint Martin d'Hères, France

E-mail : roxana.chotard@ujf-grenoble.fr, Tel. (33) 4 76 51 49 13, Fax (33) 4 76 63 54 95

Abstract

In the process of haematogenous cancer metastasis, tumor cells (TCs) must shed into the blood stream, survive in the blood circulation, migrate through the vascular endothelium (extravasation) and proliferate in the target organs. However, the precise mechanisms by which TCs penetrate the endothelial cell (EC) junctions remain one of the least understood aspects of TC extravasation. This question has generally been addressed under static conditions, despite the important role of flow induced mechanical stress on the circulating cell-endothelium interactions. Moreover, flow studies were generally focused on transient or firm adhesion steps of TC-EC interactions and did not consider TCs spreading or extravasation. In this paper, we used a parallel-plate flow chamber to investigate TC-EC interactions under flow conditions. An EC monolayer was cultured on the lower plate of the flow chamber to model the endothelial barrier. Circulating TCs were introduced into the flow channel under a well-defined flow field and TC cell shape changes on the EC monolayer were followed *in vitro* with live phase contrast and fluorescence microscopy. Two spreading patterns were observed: radial spreading which corresponded to TC extravasation, and axial spreading where TCs formed a mosaic TC-EC monolayer. By investigating the changes in area and minor/major aspect ratio, we have established a simple quantitative basis for comparing spreading modes under various shear stresses. Contrary to radial spreading, the extent of axial spreading was increased by shear stress.

1. Introduction

The major cause of death from cancer is metastatic dissemination (Tait et al., 2004), where tumor cells (TCs) locally invade and disseminate through the lymphatic system or blood circulation (Pantel and Brakenhoff, 2004). For haematogenous dissemination, TCs in the circulation must survive destruction by haemodynamic forces and host immune defenses, and then migrate out of the vessel through normal vascular endothelium (extravasation) in order to eventually proliferate in their target organs. TC extravasation plays a key role in tumor metastasis. However, the precise mechanisms by which TCs cross the endothelial cell (EC) junctions and how the presence of fluid shear forces modulates cellular responses remain poorly understood.

Leukocyte interactions with ECs have been extensively studied either under static conditions (Hashimoto et al., 2004) or under flow conditions (Carman and Springer, 2004; Cinamon et al., 2004; Kaplanski et al., 1998; Sheikh et al., 2005) and can serve as a model for interactions of circulating TCs with the vasculature (Takada et al., 1993). It is well known that shear flow has an effect on endothelial alignment and elongation (Dewey et al., 1981; Bruder et al., 2001), on cell cytoskeleton (Galbraith et al., 1998) and therefore on its local mechanical properties (Sato et al., 2000) and finally on mechanotransduction pathways (Li et al., 2005). However, TC-EC interactions have been generally addressed under static conditions in Boyden chambers (Hart et al., 2005; Li and Zhu, 1999; Roche et al., 2003) or on glass slides coated with Matrigel (Voura et al., 2001) or collagen (Longo et al., 2001).

Using a parallel-plate flow chamber, several authors have investigated the role of cell surface molecules that mediate TC adhesion under flow conditions (Tözeren et al., 1995; Haier et al., 1999; Haier and Nicolson, 2000; Kitayama et al., 2000b; Burdick et al. 2003). However, these studies were focused on transient or firm adhesion steps of TC-EC interactions and did not consider TCs spreading or extravasation. Other studies showed the importance of actin and microtubule fibers reorganization in tumor cell adhesion (Korb et al., 2004), as well as mechanotransduction effects

during metastatic adhesion of carcinoma cells, with a particular emphasis on the role of Focal adhesion kinase (Von Sengbusch et al., 2005).

More recently, Slattery et al. (2005) looked at leukocyte-facilitated TC extravasation and concluded that shear flow significantly reduced melanoma cell extravasation. In a companion paper (Dong et al., 2005), they also showed the role of Mac-1 and ICAM-1-mediated cell interactions with PMNs in human melanoma cell transmigration. However, monitoring the whole process of extravasation with live microscopy was not possible with their flow-incorporated Boyden chamber.

In this study, we used a parallel-plate flow chamber to investigate TC-EC interactions under well defined flow conditions. An EC monolayer was cultured on the lower plate of the flow chamber to model the endothelial barrier. Circulating TCs were introduced into the chamber and TC adhesion to ECs was followed *in vitro* with live phase contrast and fluorescence microscopy. TCs were distinguished from the EC monolayer by means of fluorescence labeling and their shape changes were quantified. The influence of various shear levels on TC spreading patterns was investigated.

2. Materials and methods

2.1. Cells

ECs, obtained from human umbilical veins (HUVEC), and T24 tumor cells (bladder carcinoma cell line) were cultured as previously described (Roche et al, 2003). HUVECs (passage 2 to 6) were grown to confluence on a fibronectin-coated glass slide (20 $\mu\text{g/ml}$) for 3 days (37°C, 5% CO_2 , humidified atmosphere).

T24 tumor cells were fluorescently labeled with the vital cytoplasmic dye calcein AM (7 $\mu\text{g/ml}$, Molecular Probes, USA).

2.2. Laminar flow chamber and flow assays

A parallel-plate flow chamber with a small height-to-width ratio (height $h=140\ \mu\text{m}$, width $b=14\ \text{mm}$, length $L=55\ \text{mm}$) was used as previously described (Chotard-Ghodsnia et al., 2002) and provided a fully developed (entrance length $\ll L$) two-dimensional ($h \ll b$) laminar flow ($\text{Re} < 10$).

The wall shear stress (τ_w) was independent of the position and was given by:

$$\tau_{\text{wall}} = \frac{6 \mu Q}{b h^2} \quad (1)$$

with Q the flow rate and μ the fluid viscosity. A peristaltic pump drove a constant flow rate through the circuit, consisting of a source reservoir and damping reservoir (to eliminate flow pulsatility), maintained at 5% CO₂ and 37°C. The wall shear stress was varied from 0.2±0.1 to 1.6±0.4 Pa.

2.3. Experimental protocol

The EC monolayer was first exposed to a constant shear stress of 1.6 Pa for 2 hours in order to let it recover from the stress of being inserted into the flow chamber and to better mimic physiological conditions. Shear stress induces functional changes in ECs which can modify TC adhesion on EC as reviewed by Haier and Nicolson (2001). Then, a suspension of fluorescently labeled TCs (4 million cells/ml) was perfused through the chamber. TCs were allowed to settle down and adhere to the EC monolayer for 10 minutes under static conditions. Finally, the EC-TC system was exposed to a constant shear stress (0.2, 0.8 or 1.6 Pa) for 2 hours. The integrity of the EC intercellular junctions after exposure to flow was controlled by immunostaining the EC monolayer for PECAM and VE-cadherin adhesion molecules (data not shown).

2.4. Microscopy and immunofluorescence staining

The flow chamber was placed on the stage of a phase-contrast/fluorescence microscope (Zeiss, Oberkochen, Germany) coupled to a CCD camera (Roper Scientific, Evry, France) for visualization of cell morphology *in vitro*. Phase-contrast and fluorescence images of 4 randomly selected fields were acquired every 5 minutes.

At the end of the flow assay, cells were fixed with 2% paraformaldehyde and prepared for confocal microscopy: they were permeabilized with 0.5% Triton X-100, stained with anti cytokeratin KL-1 (Serotec, France), washed three times and incubated with Alexa fluor 488-conjugated goat anti mouse IgG (Molecular Probes). Filamentous actin was revealed with Texas-red conjugated phalloidin and nuclei were stained with Hoechst 33342.

2.5. Image analysis and determination of cell shape parameters

Images were analyzed using ImageJ software (NIH Image, Bethesda, USA). Approximately 100-200 TCs from 4 randomly selected fields (each containing 30-60 cells) near the center of the flow chamber were examined for each experiment. The fraction of attached cells in each field was determined as the ratio of “TCs (per field) attached to the EC monolayer just after start-up of flow” to “TCs (per field) remaining on the EC monolayer at the end of the 10-min incubation time”.

The boundary of each cell was outlined manually from the fluorescence images. The projected area of the cell was measured as the total area enclosed by the cell boundary. The minor/major aspect ratio was measured using the “Fit Ellipse” tool. This calculates the length of the primary (major) and the secondary (minor) axes of the ellipse which best fits the selected cell (for a circular cell, minor/major=1, while for an elongated cell, minor/major tends to zero).

2.6. Statistical analysis

Student’s t-test was used to determine statistical significance ($p < 0.005$) between different experimental conditions. Data is expressed as the mean \pm SD obtained from 8 random fields observed in 2 independent experiments (4 fields per experiment) for each flow condition.

3. Results

3.1. *In vitro* model system for TC-EC interactions under shear flow

Just after the start-up of the flow, 30-50% of TCs that had settled down on the EC monolayer during the incubation period remained attached. Some of these cells rolled on the monolayer before detachment. Some others were directly located at an inter-endothelial junction where they attached firmly and began to spread. Others were located on the apical surface of an endothelial cell and had to move to an inter-endothelial junction before going through firm adhesion and spreading. Thus, time from initial TC-EC contact to the start of spreading varied widely among individual TCs. As an average, TCs traveled about 10 μm (at 0.2 Pa) to 45 μm (at 1.6 Pa) during 15 ± 5 minutes before beginning to spread (data not shown).

Representative sequences of images are shown in Figs.1-2. TCs showed two different spreading patterns on inter-endothelial junctions. About 20% of the attached TCs underwent “radial spreading”: these TCs were preferentially situated on EC tricellular corners and extended protrusions to all directions. An initially round TC with a bright hollow at its contour (Fig.1a) and intense fluorescence (Fig.1d) is shown in Fig.1. This TC spread and became less refringent (Fig.1b-1c) with weaker fluorescence (Fig.1e-1f), between $t=20$ and 45 min. The superposition of phase-contrast (Fig.1a-1c) and fluorescence (Fig.1d-1f) images suggests that this TC migrated through the inter-endothelial junction and became laterally overlaid by the adjacent ECs.

Another 20% of the attached TCs underwent “axial spreading”: these TCs spread along the inter-endothelial axis between two adjacent ECs and intermingled with these ECs (Fig.2a-2c). Fluorescence images clearly showed the axial spreading pattern (Fig.2d-2f): at $t=45$, TCs remained elongated in between the ECs which slightly overlaid the TC lateral borders (Fig.2c, Fig.2f).

The rest of attached TCs either remained round or detached some time after the start-up of flow, or were part of a TC aggregate and could not be followed any longer.

3.2. Morphological analysis of spreading patterns

As some TCs began to spread earlier than others, the image fields contained round cells and cells with different extents of spreading. To characterize the time-dependent evolution of TC morphology, we plotted data with a synchronized time, i.e. time zero refers to the spreading start time for each cell.

Fig.3 shows the TCs average projected area as a function of synchronized time for both axial and radial spreading patterns under a shear stress of 1.6 Pa. As cells spread axially or radially, their area increased similarly with time and reached a steady state. The maximum area of a spread TC ($1707 \mu\text{m}^2$ for radial and $1540 \mu\text{m}^2$ for axial) was approximately 4 times larger than its initial area ($360 \mu\text{m}^2$ for a round TC). Axial and radial initial area increase rate ($40 \mu\text{m}^2/\text{min}$) and the maximum value of the area were similar at 1.6 Pa. Also shown is the data corresponding to TC

spreading on a plain fibronectin-coated glass slide (control substrate). In these conditions, nearly all attached TCs underwent radial spreading. No axial spreading was observed. The extent of TC radial spreading on fibronectin was similar to that on the EC monolayer. However, the spreading rate on fibronectin ($108 \mu\text{m}^2/\text{min}$) was higher than the rate on the EC monolayer ($40 \mu\text{m}^2/\text{min}$).

As the cell area could not discriminate between these two morphologically different populations, we used another morphometrical parameter.

The average minor/major aspect ratio of spreading cells was plotted against time at 1.6 Pa (Fig.4). This parameter remained constant for radially spreading TCs (0.80) whereas it decreased from 0.82 ($t=0$) to a nearly constant value of 0.54 (between $t=20$ and $t=60$ min) for axially spreading TCs. After 60 min, the ratio for axially spreading cells began to increase slightly, while these cells inserted themselves into the EC monolayer. Moreover, the minor/major ratio of TCs on fibronectin-coated glass slide remained constant (0.90), confirming their radial spreading pattern.

3.3. Influence of shear flow on cell shape

The percentage of TCs attached on the EC monolayer significantly decreased (from 50% to 30%, $p<0.005$) when the shear flow increased from 0.2 to 0.8 or 1.6 Pa (Fig.5). Approximately the same percentage of attached TCs underwent radial (15% to 19%) or axial (12% to 22%) spreading, independently of the level of shear stress.

We next analyzed the influence of shear flow on TC spreading kinetics. For radially spreading TCs (Fig.6a), neither the area nor its rate of increase was changed by increasing the shear stress. The plateau was reached after $t=60$ min independently of the shear stress level. For axially spreading TCs (Fig.6b), the rate of area increase was not affected by shear stress. However, the plateau area was significantly ($p<0.005$) enhanced at 0.8 and 1.6 Pa (respectively: $1593 \mu\text{m}^2$ and $1540 \mu\text{m}^2$) compared to 0.2 Pa ($1014 \mu\text{m}^2$). Moreover, the plateau for axially spreading TCs at 0.2 Pa was reached earlier ($t=40$ min) than at 0.8 or 1.6 Pa ($t=60$ min).

In order to exhibit a single graph differentiating the two populations under flow, we plotted the average minor/major ratio versus mean area at 0.2 Pa and 1.6 Pa shear stresses (Fig.7). The “minor/major versus area” trajectory was horizontal, independently of the shear stress level, for radially spreading TCs. Their shape nearly corresponded to a circle whose radius increased from 11 μm (at time zero) to 24 μm (at 70 min). This trajectory followed a decreasing trend for axially spreading TCs which was nevertheless shorter at 0.2 Pa than at 1.6 Pa. Indeed, the increase of the applied shear stress did not affect the maximum elongation of axially spread TCs but significantly ($p < 0.001$) increased their maximum area.

3.4. Spatial localization of spread TCs within the EC monolayer

We further analyzed the spatial arrangement of TCs within the EC monolayer by confocal microscopy on a fixed sample after exposure to flow, for both axially and radially spread TCs. TCs were specifically labelled using a cytokeratin antibody, KL-1. Filamentous actin and nuclei were also visualized for both cell types.

Confocal stacks showing typical TCs undergoing radial spreading (Fig.8a-c) and axial spreading (Fig.8d-f) on the EC monolayer are shown at 1.6 Pa. For the radially spread TC, actin filaments of adjacent ECs overlay the TC external borders. In contrast, for the axially spread TC, lateral borders are in close contact with adjacent ECs. The upper sketches give a tentative representation of the TCs position relative to the EC monolayer, with a TC underneath the EC monolayer in the case of radial spreading, and an axially spread cell simply intermingled with the ECs.

4. Discussion

In this study, we have developed an *in vitro* model which allows live phase contrast and fluorescent visualization of TC spreading on an EC monolayer. We focused on TCs morphology as they interact with the EC monolayer under controlled flow levels.

The influence of shear flow on ECs and TCs has been studied by several authors: ECs elongate and reorient in the direction of flow (Dewey et al., 1981; Bruder et al., 2001). Their stress fibers and microtubules align in the direction of flow (Galbraith et al., 1998). This reorganization depends on several intracellular signaling networks (Hu et al., 2002; Li et al., 2005). It is tempting to speculate that the appearance of TC alignment involves the formation of stress fibers which allow better anchoring of TCs and better resistance to flow-induced shear forces. Korb et al. (2004) showed that HT29 colon carcinoma cells adherent on collagen IV or laminin-coated substrate, remained rounded (with reduced stress fibers) but showed enlarged and hyperphosphorylated focal adhesions under 0.2 Pa shear stress as compared to static conditions. Following this work, it is planned to study the reorganization of stress fibers and focal adhesions of TCs under well defined flow conditions, in the two cases of spreading (i.e. radial and axial).

In addition to altering the morphological features of cells, shear stress also has an effect on their mechanical properties. Sato et al. (2000) showed that the stiffness was higher on the upstream side than on the downstream of ECs sheared at 2 Pa for 6 hours. The cytoskeletal components should be involved in such morphological behavior as suggested by Haier and Nicolson (2001). These authors showed that the integrity of actin fibers and microtubules can modulate TC adhesion *in vivo* and *in vitro*. They suggested that changes in cell deformability and avidity of cell adhesion molecules after disruption of cytoskeletal components play an important role for initial adhesive interactions of TCs within the hepatic microcirculation (Korb et al., 2004).

Our data (Fig.5a) show that the percentage of attached TCs on the EC monolayer was shear-dependent: 50% of TCs remained attached under 0.2-Pa versus 30% under 1.6-Pa shear stress. This is in agreement with detachment assays carried out on colon carcinoma cells (Burdick et al., 2003). We have not tried to identify the molecules involved, but it is known that attachment of TCs to ECs can be mediated by adhesive proteins such as E-selectin and β 1-integrins (Haier et al., 1999, Burdick et al., 2003). Furthermore, as shown by Dong et al. (2005), tumor cell attachment to an EC monolayer under shear stress can be enhanced in the presence of polymorphonuclears (PMNs),

which would act as binding mediators between melanoma cells and ECs. PMNs express β_2 -integrins (Mac-1 and LFA-1) which can bind to both the ICAM-1 expressing TCs and ECs (Slattery et al., 2005). Further analysis is needed to elucidate such adhesive interactions in our experiments.

Mechanotransduction phenomena similar to those pertaining to ECs under shear flow may also influence TC behavior. For example, hydrodynamic shear forces can increase Tyr-phosphorylation of Focal Adhesion Kinase (FAK), which is one of the most important components of the integrin-linked focal contacts (Von Sengbusch et al., 2005). These authors suggested that FAK is not only involved in “early events” of integrin mediated TC “adhesion” under dynamic conditions, but is also responsible for the establishment of “stabilized adhesive interactions”, which enable TCs to resist shear forces within the microcirculation of target organs. Further analyses must be performed to verify if FAK modulates other TC adhesive interactions, such as “spreading”, under flow conditions.

After initial adhesion, we observed that TCs started to move to intercellular endothelial junctions before beginning to spread. This agrees with observations by Longo et al. (2001) under static conditions, in the case of melanoma cells. Following this initial migration, TCs showed two different spreading patterns: radial spreading and axial spreading. To our knowledge, this is the first time that such two behaviors are observed in a single experiment. The same number of cells was found to spread radially or axially (Fig.5b). In addition, the shear stress had no effect on the percentage (20%) of attached TCs undergoing radial or axial spreading. Cinamon et al. (2003) showed similar results for leukocytes whose transendothelial migration was independent of the shear flow magnitude.

TCs which spread radially (Fig.1a-f) were found underneath the EC monolayer after one hour. This location of TCs below the monolayer was confirmed by confocal microscopy (Fig.8). This suggests that radial spreading corresponds to a transendothelial migration of TCs. This phenomenon preferentially occurred at EC tricellular corners (Fig.1a-c), as already shown for transmigrating neutrophils (Burns et al., 1997). In our model, the transendothelial migration of T24 bladder

carcinoma cells is slower (1 hour) than that of leukocytes (a few minutes) (Cinamon and Alon, 2003). Melanoma cell transendothelial migration under static conditions was also slower (Voura et al., 1998). These authors suggested that TCs require more time to transmigrate because an EC retraction is needed, whereas leukocytes are able to squeeze through inter-endothelial junctions without inducing EC retraction (Cinamon and Alon, 2003). In our conditions, the size of TCs (15-20 μm) could be a limiting factor, which could impose either a retraction of ECs, or/and an important squeezing of TCs. Both phenomena require a reorganisation of cell shapes which would explain the delay in cell extravasation. Moreover, the rheological properties (i.e. elastic modulus) of transmigrating cells have been found to be quite larger in the case of tumor cells (carcinoma cells, 3800 Pa, Goldmann & Ezzell, 1996; cancerous human bladder cells, 800-1000 Pa, Lekka et al., 1999) as compared to leukocytes (human neutrophil, 30 Pa, Dong et al., 1988; Sung et al., 1988). In addition, their ability to communicate with ECs probably modulates the time course of cell transmigration.

In our experiments, the rate and extent of radial spreading were not affected by the shear stress (Fig.3). This might be related to the fact that the apical surface of radially spread TCs was covered by surrounding ECs and consequently was not under the direct influence of the shear stress. A similar phenomenon was observed by Kitayama et al. (2000a) for transmigrating monocytes.

TCs which spread axially (Fig.2a-f) were located at the junction between two ECs. They spread longitudinally along the EC-EC contact axis, were not covered by neighbouring ECs (Fig.8) and formed a mosaic monolayer. Different tumor cell lines are able to form mosaic linings during their transendothelial migration under static or flow conditions both *in vitro* and *in vivo* (Longo et al., 2001; Al-Mehdi et al, 2000). TCs which insert into the EC monolayer could act as the seeds of secondary tumors. The axial spreading pattern was apparently induced by the presence of ECs, since such a morphology was never observed in the control experiments on a fibronectin-coated substrate, in the absence of ECs. Our observations of the inclusion of TCs into the EC monolayer needs further investigations, in particular on the role of intercellular adhesion molecules such as

cadherins, which might be involved in the EC-TC cell junctions. Cadherins are involved in cell-cell junctions; N-cadherin has been shown to be involved in the transmigration of melanoma cells through the endothelium (Qi et al., 2005) and VE-cadherin is expressed by highly aggressive melanoma cells (Hendrix et al., 2001). The presence of mosaic vessels with both ECs and TCs forming the luminal surface has already been observed in mouse models of colon carcinoma (Chang et al., 2000), but in a recent publication, it was found that in some cases, the endothelial cell lining were present but lacked endothelial cell markers (di Tomaso et al., 2005).

The rate of axial spreading was not affected by the increase of shear stress, but the extent of spreading was enhanced by the shear flow. This is consistent with the work of Coughlin and Schmid-Schönbein (2004) who showed that leukocyte lamellipodium formation increased with the amplitude and duration of shear stress. In our study, however, there seems to be a shear stress threshold (0.8 Pa) above which there is no increase in spreading area, since the two higher shear stresses (0.8 and 1.6 Pa) resulted in similar plateaus. The increase of axial spreading with shear stress may be a way for TCs to better resist to higher detachment forces, as suggested by Dong and Lei (2000) both theoretically and experimentally. Using a 2D model, they showed that, due to shear flow-induced cell deformation, the cell-substrate contact area is increased twice when the shear stress goes from 0.05 to 2 Pa, leading to an increased adherence.

To summarize, this work has shown the appearance of two different TC spreading mechanisms on EC monolayer and clearly identified them: radial spreading, leading to extravasation, and axial spreading, leading to the formation of a mosaic cell monolayer. As expected, the effect of shear changed the initial number of adhering cells, but it was found to enhance only axial spreading. Further investigations are needed, in particular on the interrelations between the shear modulation of TC mechanical properties with intracellular structural elements, TC mechanotransduction and the role of adhesion molecules in these phenomena.

Acknowledgements

This work has been supported partly by “La ligue contre le cancer” and the RTN project funded by the EU, Contract N° CT- 2000-00105. We thank Alexei Grichine for his assistance with the confocal microscope.

References

- Al-Mehdi, A.B., Tozawa, K., Fisher, A.B., Shientag, L., Lee, A., and Muschel, R.J., 2000. Intravascular origin of metastasis from the proliferation of endothelium-attached tumor cells: a new model for metastasis. *Nat. Med.* 6, 100-102.
- Bruder, J.L., Hsieh, T-C., Lerea, K.M., Olson, S.C., Wu, J.M., 2001. Induced cytoskeletal changes in bovine pulmonary artery endothelial cells by resveratrol and accompanying modified responses to arterial shear stress. *BMC Cell Biology* 2, 1.
- Burdick, M.M., McCaffery, J.M., Kim, Y.S., Bochner, B.S., Konstantopoulos, K., 2003. Colon carcinoma cell glycolipids, integrins, and other glycoproteins mediate adhesion to HUVECs under flow. *Am. J. Physiol. Cell Physiol.* 284, 977-987.
- Burns, A.R., Walker, D.C., Brown, E.S., Thurmon, L.T., Bowden, R.A., Keese, C.R., Simon, S.I., Entman, M. L., Smith, C.W., 1997. Neutrophil transendothelial migration is independent of tight junctions and occurs preferentially at tricellular corners. *J. Immunol.* 159, 2893-2903.
- Carman, C.V. and Springer, T.A., 2004. A transmigratory cup in leukocyte diapedesis both through vascular endothelial cells and between them. *J. Cell Biol.* 167, 377-388.
- Chang, Y.S., di Tomaso, E., McDonald, D.M., Jones, R., Jain, R.K., Munn, L.L., 2000. Mosaic blood vessels in tumors: frequency of cancer cells in contact with flowing blood. *Proc. Natl. Acad. Sci. U.S.A.* 97, 14608-14613.
- Chotard-Ghodsniya, R., Drochon, A., Grebe, R., 2002. A new flow chamber for the study of shear stress and transmural pressure upon cells adhering to a porous biomaterial. *J. Biomech. Eng.* 124: 258-261.
- Cinamon, G. and Alon, R., 2003. A real time in vitro assay for studying leukocyte transendothelial migration under physiological flow conditions. *J Immun. Meth.* 273, 53-62.
- Cinamon, G., Shinder, V., Shamri, R., Alon, R., 2004. Chemoattractant signals and β 2 occupancy at apical endothelial contacts combine with shear stress signals to promote transendothelial neutrophil migration. *J. Immunol.* 173, 7282-7291.
- Coughlin, M.F. and Schmid-Schönbein, G.W., 2004. Pseudopod projection and cell spreading of passive leukocytes in response to fluid shear stress. *Biophys J.* 87, 2035-2042.
- Dewey Jr., C.F., Bussolari, S.R., Gimbrone Jr., M.A., Davies, P.F., 1981. The dynamic response of vascular endothelial cells to fluid shear stress. *J. Biomech. Eng.* 103, 177-185.
- di Tomaso, E., Capen, D., Haskell, A., Hart, J., Logie, J.J., Jain, R.K., McDonald, D.M., Jones, R., Munn, L.L., 2005. Mosaic Tumor Vessels: Cellular Basis and Ultrastructure of Focal Regions Lacking Endothelial Cell Markers. *Cancer Res.* 65, 5740-5749.
- Dong, C., Skalak, R., Sung, K.L., Schmid-Schonbein, G.W., Chien, S., 1988. Passive deformation analysis of human leukocytes. *J. Biomech. Eng.* 110, 27-36.
- Dong, C., Lei, X.X., 2000. Biomechanics of cell rolling: shear flow, cell-surface adhesion, and cell deformability. *J. Biomech.* 33, 35-43.
- Dong, C., Slattery, M., Liang, S., 2005. Micromechanics of tumor cell adhesion and migration under dynamic flow conditions. *Frontiers in Bioscience* 10, 379-384.

- Galbraith, C.G., Skalak, R., Chien, S., 1998. Shear stress induces spatial reorganization of the endothelial cell cytoskeleton. *Cell Motility & the Cytoskeleton* 40, 317-330.
- Goldmann, W.H., Ezzell, R.M. 1996. Viscoelasticity in wild-type and vinculin-deficient (5.51) mouse F9 embryonic carcinoma cells examined by atomic force microscopy and rheology. *Exp. Cell Res.* 226, 234-237.
- Haier, J., Nasralla, M.Y., Nicolson, G.L., 1999. β 1-integrin-mediated dynamic adhesion of colon carcinoma cells to extracellular matrix under laminar flow. *Clinical & Experimental Metastasis* 17, 377-387.
- Haier, J. and Nicolson, G.L., 2000. Tumor cell adhesion of human colon carcinoma cells with different metastatic properties to extracellular matrix under dynamic conditions of laminar flow. *J. Cancer Res. Clin. Oncol.* 126, 699-706.
- Haier, J. and Nicolson, G.L., 2001. Tumor cell adhesion under hydrodynamic conditions of fluid flow. *APMIS* 109, 241-262.
- Hart, C.A., Brown, M., Bagley, S., Sharrard, M., Clarke, N.W., 2005. Invasive characteristics of human prostatic epithelial cells: understanding the metastatic process. *Br. J. Cancer* 92, 503 – 512.
- Hashimoto, K., Kataoka, N., Nakamura, E., Asahara, H., Ogasawara, Y., Tsujioka, K., Kajiya, F., 2004. Direct observation and quantitative analysis of spatiotemporal dynamics of individual living monocytes during transendothelial migration, *Atherosclerosis* 177, 19–27.
- Hendrix, M.J., Seftor, E.A., Meltzer, P.S., Gardner, L.M., Hess, A.R., Kirschmann, D.A., Schattman, G.C., Seftor, R.E., 2001. Expression and functional significance of VE-cadherin in aggressive human melanoma cells: role in vasculogenic mimicry. *Proc. Natl. Acad. Sci. U.S.A.* 98, 8018-8023.
- Hu, Y-L., Li, S., Miao, H., Tsou, T.C., Angel del Pozo, M., Chien, S., 2002. Roles of microtubule dynamics and small GTPase rac in endothelial cell migration and lamellipodium formation under flow. *J. Vasc. Res.* 39, 465-476.
- Kaplanski, G., Marin, V., Fabrigoule, M., Boulay, V., Benoliel, A.M., Bongrand, P., Kaplanski, S., Farnarier, C., 1998. Thrombin-activated human endothelial cells support monocyte adhesion in vitro following expression of intercellular adhesion molecule-1 (ICAM-1; CD54) and vascular cell adhesion molecule-1 (VCAM-1; CD106). *Blood* 92, 1259-1267.
- Kitayama, J., Hidemura, A., Saito, H., Nagawa, H., 2000a. Shear stress affects migration behaviour of polymorphonuclear cells arrested on endothelium. *Cellular Immunology* 203, 39-46.
- Kitayama, J., Tsuno, N., Sunami, E., Osada, T., Muto, T., Nagawa, H., 2000b. E-selectin can mediate the arrest type adhesion of colon cancer cells under physiological shear flow. *Eur. J. Cancer.* 36, 121-127.
- Korb, T., Schlüter, K., Enns, A., Spiegel, H-U., Senninger, N., Nicolson, G.L., Haier, J., 2004. Integrity of actin fibers and microtubules influences metastatic tumor cell adhesion. *Exp. Cell Res.* 299, 236-247.
- Lekka, M., Laidler, P., Gil, D., Lekki, J., Stachura, Z., Hryniewicz, A.Z. 1999. Elasticity of normal and cancerous human bladder cells studied by scanning force microscopy. *Eur Biophys. J.* 28, 312-316.
- Li, Y., Zhu, C., 1999. A modified Boyden chamber assay for tumour cell transendothelial migration in vitro. *Clin. Exp. Metastasis* 17, 423-429.
- Li, Y-S.J., Haga, J.H., Chien, S., 2005. Molecular basis of the effects of shear stress on vascular endothelial cells. *J. Biomechanics* 38, 1949-1971.
- Longo, N., Yanez-Mo, M., Mittelbrunn, M., de la Rosa, G., Munoz, M-L., Sanchez-Madrid, F., Sanchez-Mateos, P., 2001. Regulatory role of tetraspanin CD9 in tumor-endothelial cell interaction during transendothelial invasion of melanoma cells. *Blood* 98, 3717-3726.
- Pantel, K., Brakenhoff, R.H., 2004. Dissecting the metastatic cascade. *Nat. Rev. Cancer* 4, 448-456.
- Qi, J., Chen, N., Wang, J., and Siu, C.H., 2005. Transendothelial Migration of Melanoma Cells Involves N-Cadherin-mediated Adhesion and Activation of the β -Catenin Signaling Pathway. *Mol. Biol. Cell* 16, 4386-4397.
- Roche, Y., Pasquier, D., Rambeaud, J-J., Seigneurin, D., Duperray, A., 2003. Fibrinogen mediates bladder cancer cell migration in an ICAM-1-dependent pathway. *Thromb. Haemost.* 89, 1089-1097.

- Sato, M., Nagayama, K., Kataoka, N., Sasaki, M., Hane, K., 2000. Local mechanical properties measured by atomic force microscopy for cultured bovine endothelial cells exposed to shear stress. *J. Biomechanics* 33, 127-135.
- Sheikh, S., Rahman, M., Gale, Z., Luu, N.T., Stone, P.C., Matharu, N.M., Rainger, G.E., Nash, G.B., 2005. Differing mechanisms of leukocyte recruitment and sensitivity to conditioning by shear stress for endothelial cells treated with tumour necrosis factor-alpha or interleukin-1beta. *Br J Pharmacol.* 145, 1052-1061.
- Slattery, M.J., Liang, S., Dong, C., 2005. Distinct role of hydrodynamic shear in leukocyte-facilitated tumor cell extravasation. *Am. J. Physiol. Cell Physiol.* 288, C831-C839.
- Sung, K.L., Dong, C., Schmid-Schonbein, G.W., Chien, S., Skalak, R., 1988. Leukocyte relaxation properties. *Biophys. J.* 54, 331-336.
- Tait, C.R., Dowell, D. and Horgan, K., 2004. Do metastases metastasize? *J. Pathol.* 203, 515-518.
- Takada, A., Ohmori, K., Yoneda, T., Tsuyuoka, K., Hasegawa, A., Kiso, M., Kannagi, R., 1993. Contribution of carbohydrate antigens sialyl Lewis A and sialyl Lewis X to adhesion of cancer cells to endothelium, *Cancer Res.* 53, 354-361.
- Tözeren, A., Kleinman, H.K., Grant, D.S., Morales, D., Mercurio, A.M., Byers, S.W., 1995. E-selectin-mediated dynamic interactions of breast- and colon cancer- cells with endothelial-cell monolayers. *Int. J. Cancer* 60, 426-431.
- Von Sengbusch, A., Gassmann, P., Fisch, K.M., Enns, A., Nicolson, G.L., Haier, J., 2005. Focal adhesion kinase regulates metastatic adhesion of carcinoma cells within liver sinusoids. *Am. J. Pathol.* 166, 585-596.
- Voura, E.B., Ramjeesingh, R.A., Montgomery, A., Siu, C-H., 2001. Involvement of integrin $\alpha_v\beta_3$ and cell adhesion molecule L1 in transendothelial migration of melanoma cells. *Molecular Biology of the Cell* 12, 2699-2710.
- Voura, E.B., Sandig, M., Kalnins, V.I., Siu, C-H., 1998. Cell shape changes and cytoskeleton reorganization during transendothelial migration of human melanoma cells. *Cell Tissue Res.* 293, 375-387.

Caption for figures

Fig.1. Radial spreading of TCs under flow (shear stress = 1.6 Pa) observed using phase contrast (a-c) and fluorescence (d-f) microscopy at $t=0$ (a,d), $t=20$ min (b,e) and $t=45$ min (c,f) after injection of TCs on the EC monolayer. The fluid flow is oriented from right to left of the images.

Fig.2. Axial spreading of TCs under flow (shear stress = 1.6 Pa) observed using phase contrast (a-c) and fluorescence (d-f) microscopy at $t=0$ (a,d), $t=20$ min (b,e) and $t=45$ min (c,f) after injection of TCs on the EC monolayer. The fluid flow is oriented from right to left of the images.

Fig.3. Time course of TCs projected area evolution for radial and axial spreading on an EC monolayer under a shear stress of 1.6 Pa. Results are shown as mean \pm SD ($n=19$ for radial and 22 for axial TCs). Dotted line: radial spreading of TCs on fibronectin-coated glass slide ($n=20$).

Fig.4. Time course of TCs minor/major aspect ratio for radial (triangles) and axial (squares) spreading on an EC monolayer under a shear stress of 1.6 Pa. Results are shown as mean \pm SD ($n=19$ for radial and 22 for axial TCs). Dotted line: radial spreading of TCs on fibronectin-coated glass slide ($n=20$). Inset illustrates the best fitting ellipse defining the major and minor axes for a selected cell. * indicates statistical significance ($p<0.005$) of axial compared to radial aspect ratio from $t=20$ to $t=70$ min.

Fig.5. Effect of shear flow on the number of TCs: a) % attached TCs on the EC monolayer (relative to the number of TCs remaining on the EC monolayer at the end of the 10-min incubation time, which corresponds to a total number of 309, 362 and 379 TCs observed at 0.2, 0.8 and 1.6 Pa, respectively), b) % TCs undergoing radial or axial spreading (relative to the initial number of attached cells). Results are shown as mean \pm SD from 8 random fields observed in two independent experiments for each flow rate. The numbers over each bar correspond to the total number of cells observed in each case. * indicates statistical significance ($p < 0.005$) of % attached TCs at 0.8 and 1.6 Pa as compared to 0.2 Pa.

Fig.6. Effect of shear flow on the evolution of TCs projected area: (a) radial spreading, no significant difference is found between the different shear levels. (b) axial spreading, the cell area at 0.2 Pa is significantly lower than at 0.8 and 1.6 Pa ($p < 0.005$) from $t = 20$ to $t = 120$ min. Results are shown as mean \pm SD for each applied shear stress.

Fig.7. Minor/major ratio versus area (trajectory) for the two spreading patterns at two different shear stresses, from $t = 0$ to 70 min.

Fig.8. Confocal series showing typical TCs undergoing: radial spreading (a-c), axial spreading (d-f) on an EC monolayer at 1.6 Pa shear stress for 30 min. Fixed cells were stained for TCs cytokeratin (b,e), actin fibers (c,f) and nuclei (a,d). Individual images are shown in an apical-to-basal direction. $Z = 0 \mu\text{m}$ corresponds to the first section as illustrated in the upper sketch. In (a-c), actin filaments of adjacent ECs clearly overlay external borders of the radially spread TC (arrowheads). In (d-f), lateral borders of an axially spread TC are in close contact with adjacent ECs (arrows). N corresponds to TC nuclei.

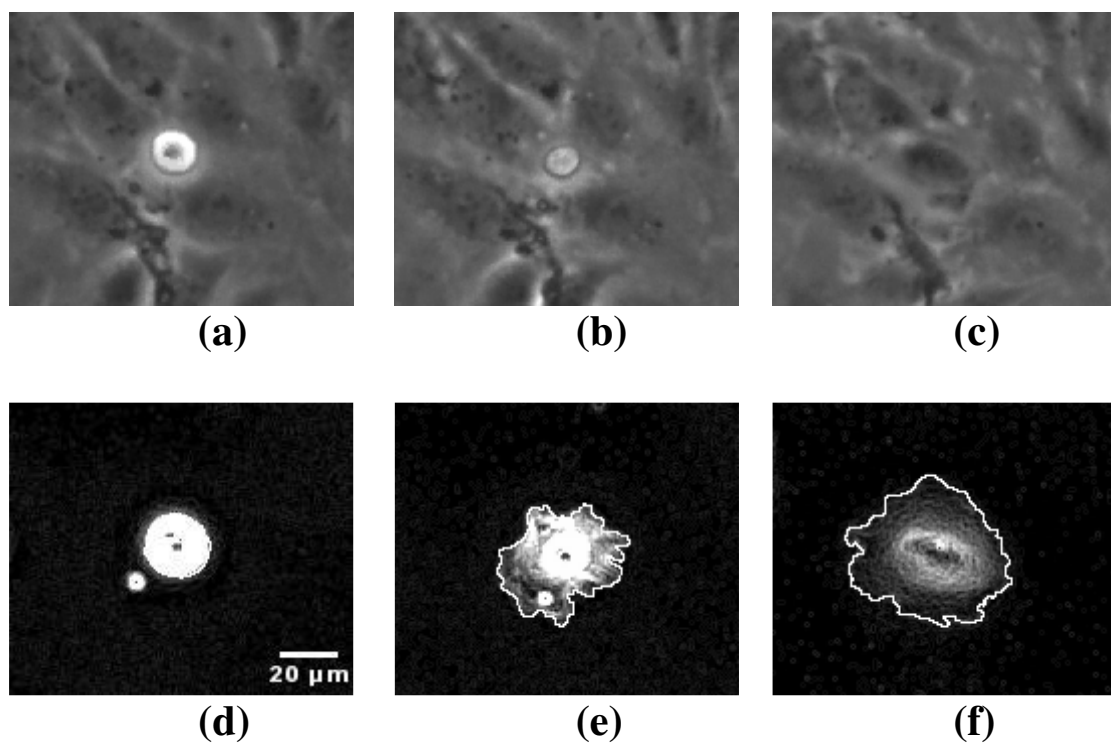
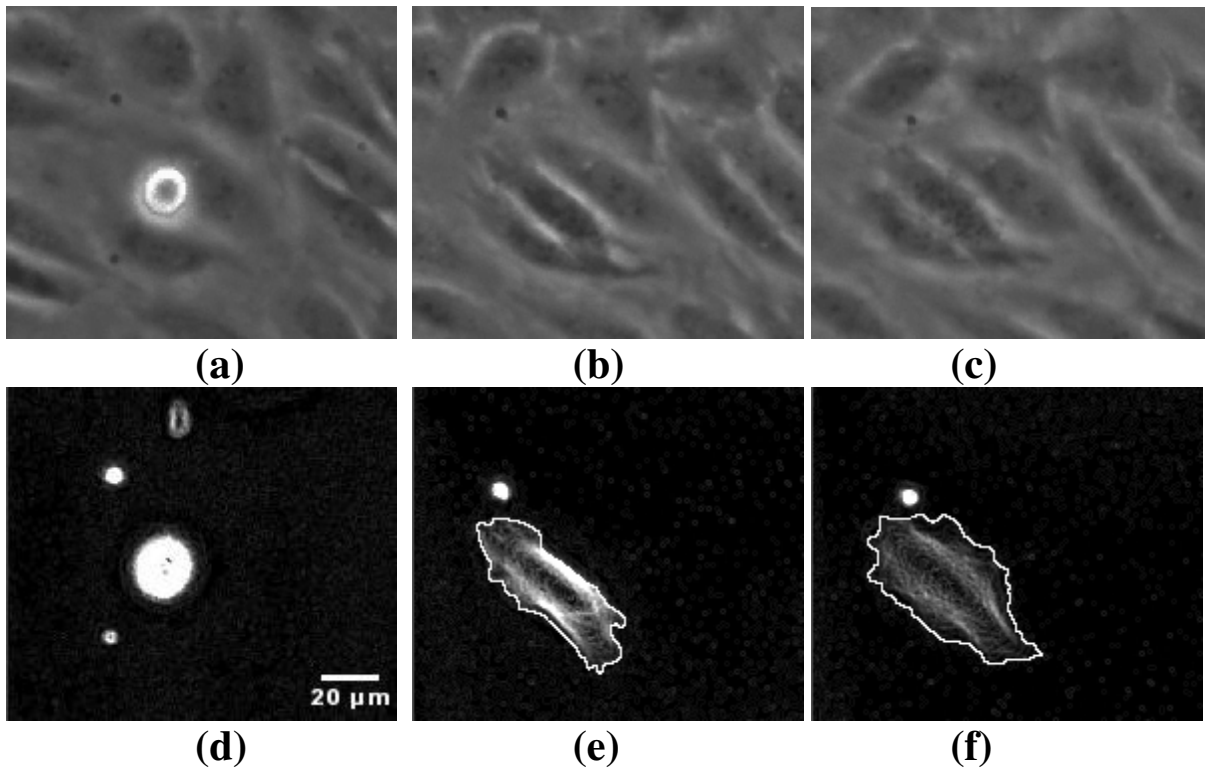


Fig.1

**Fig. 2**

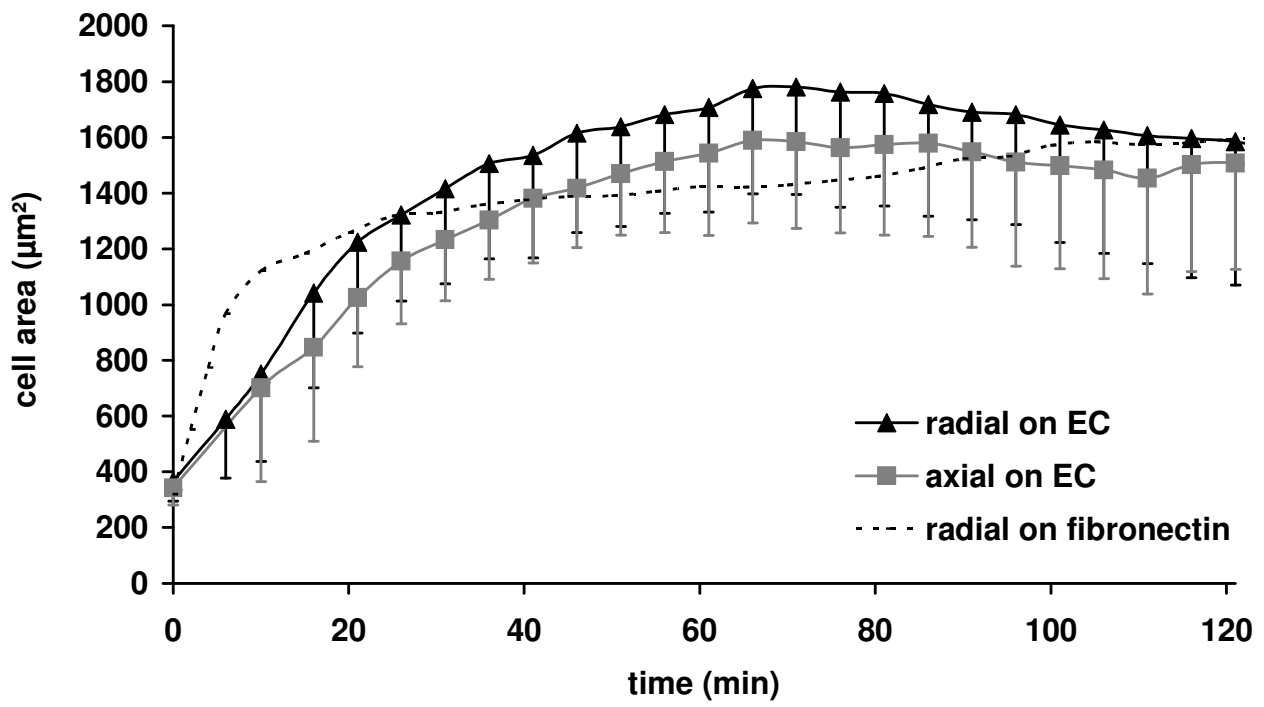


Fig. 3

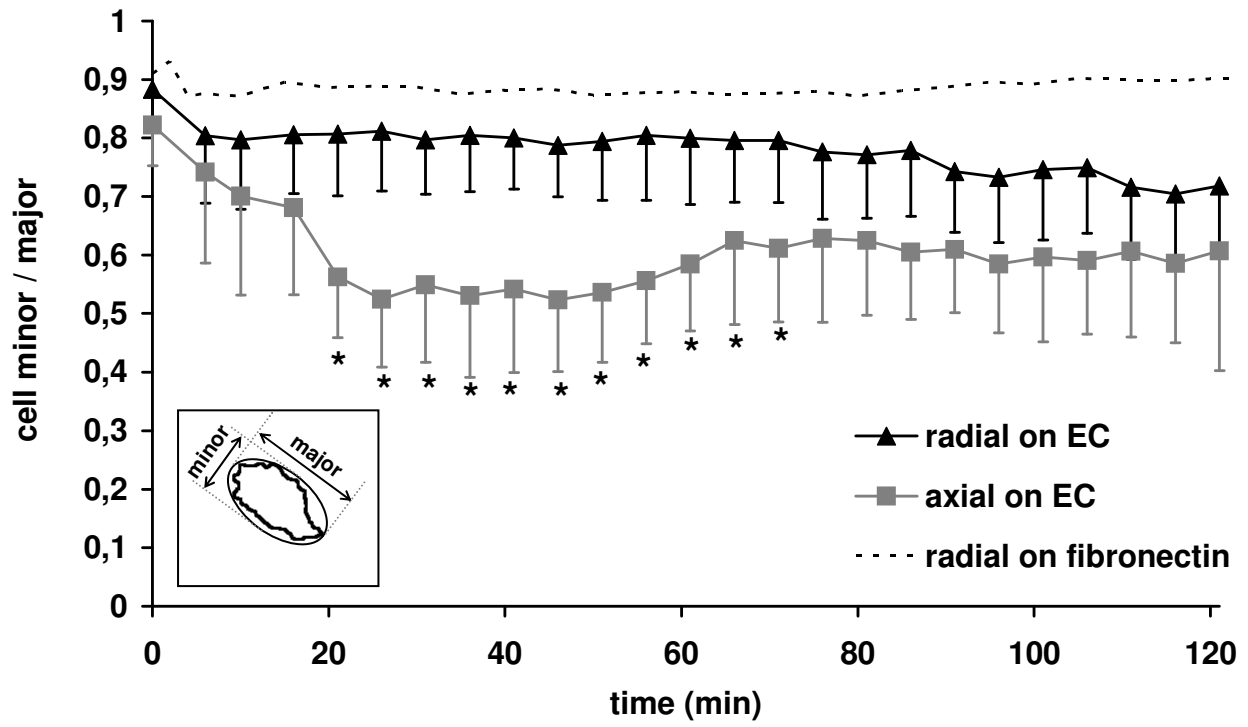


Fig. 4

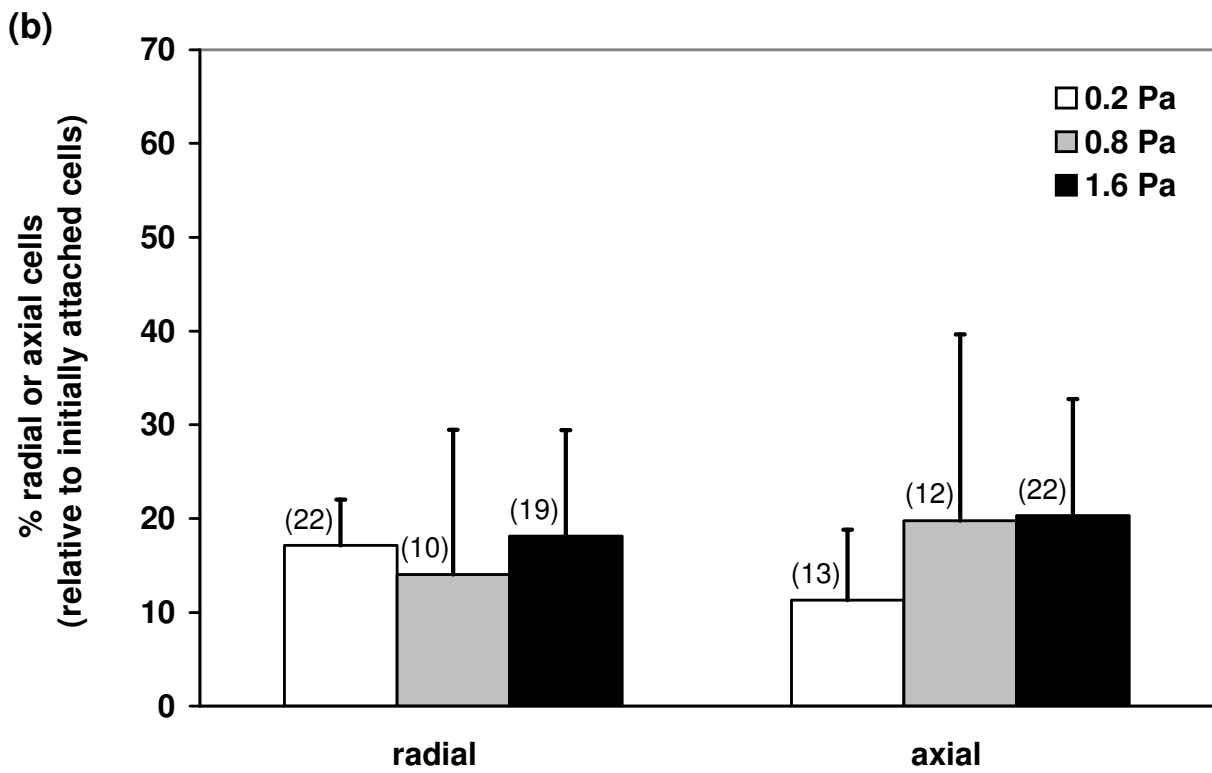
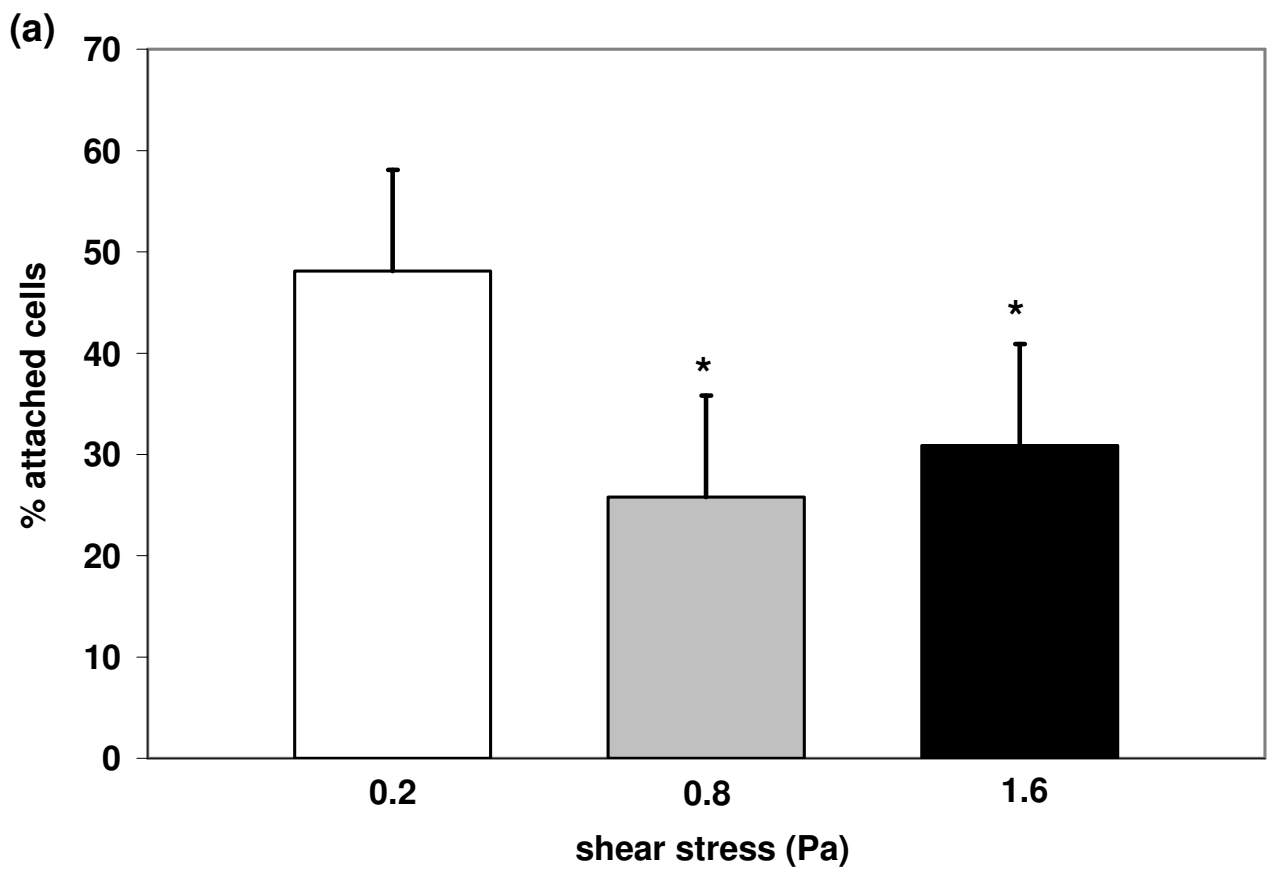


Fig. 5

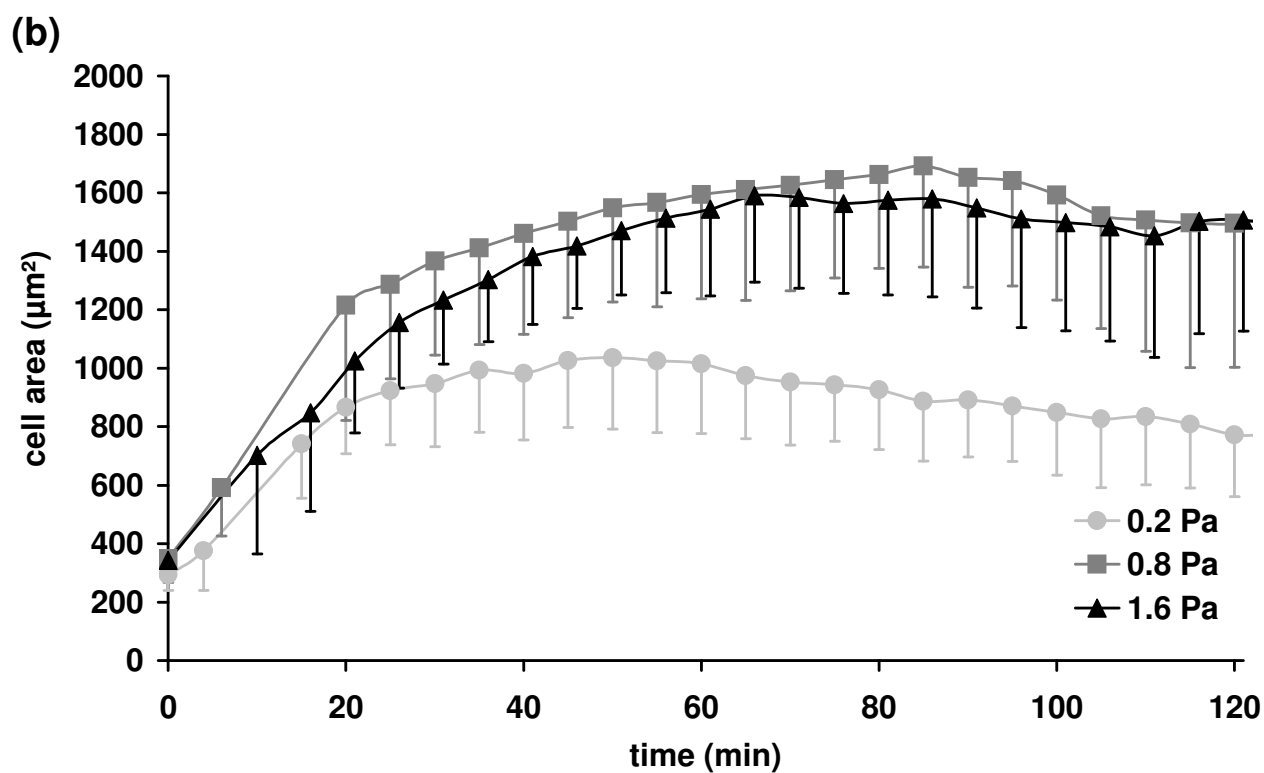
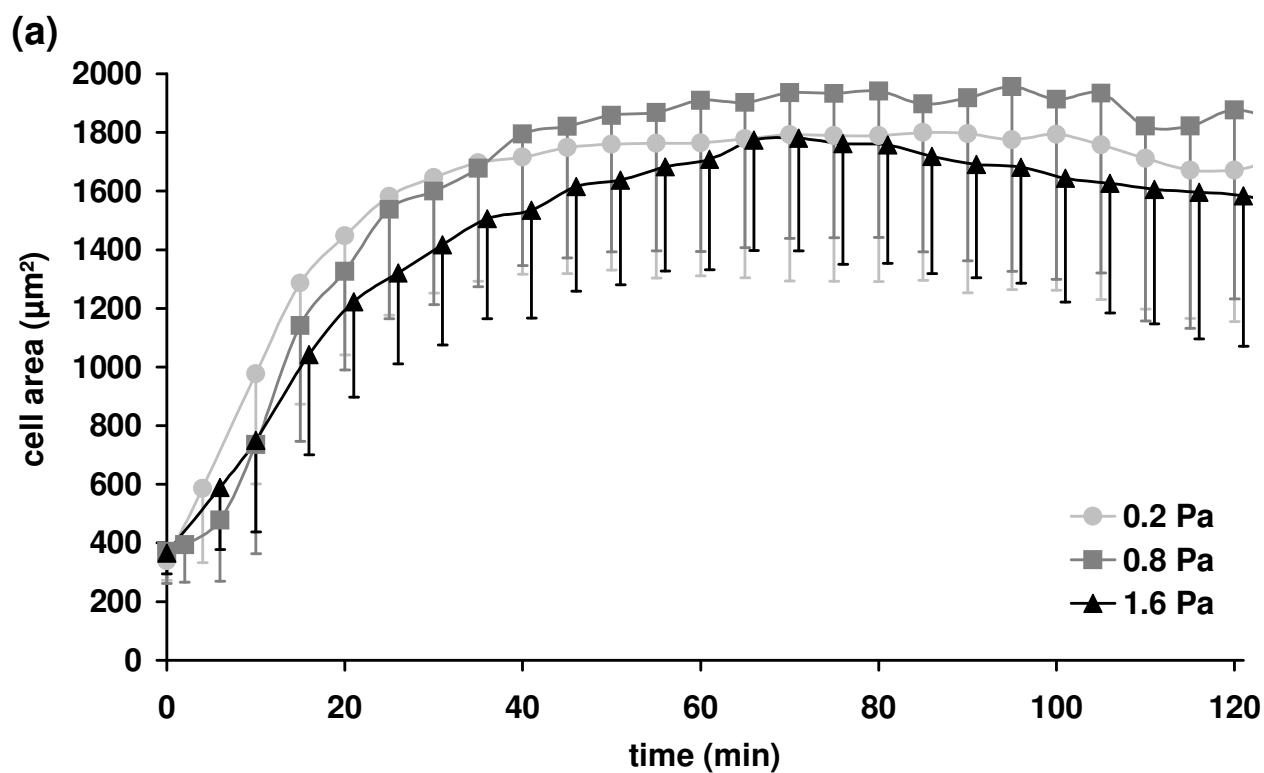


Fig. 6

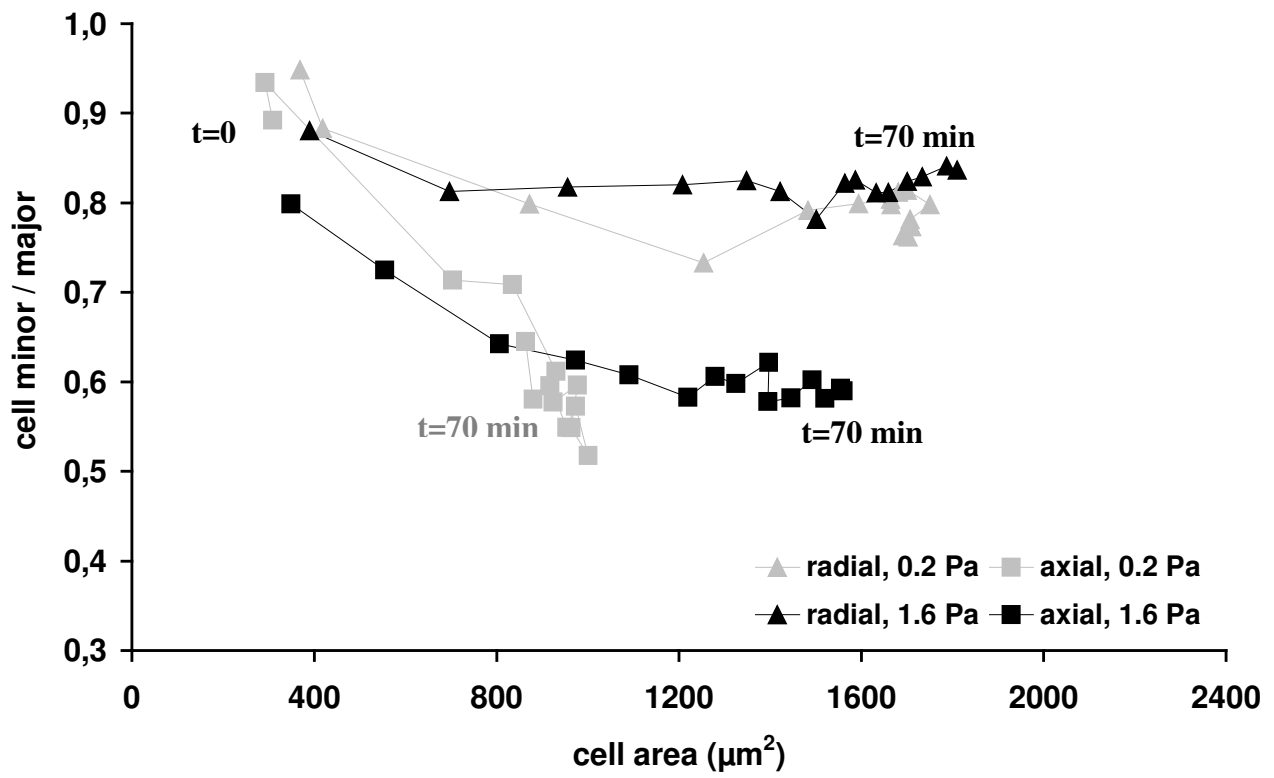


Fig. 7

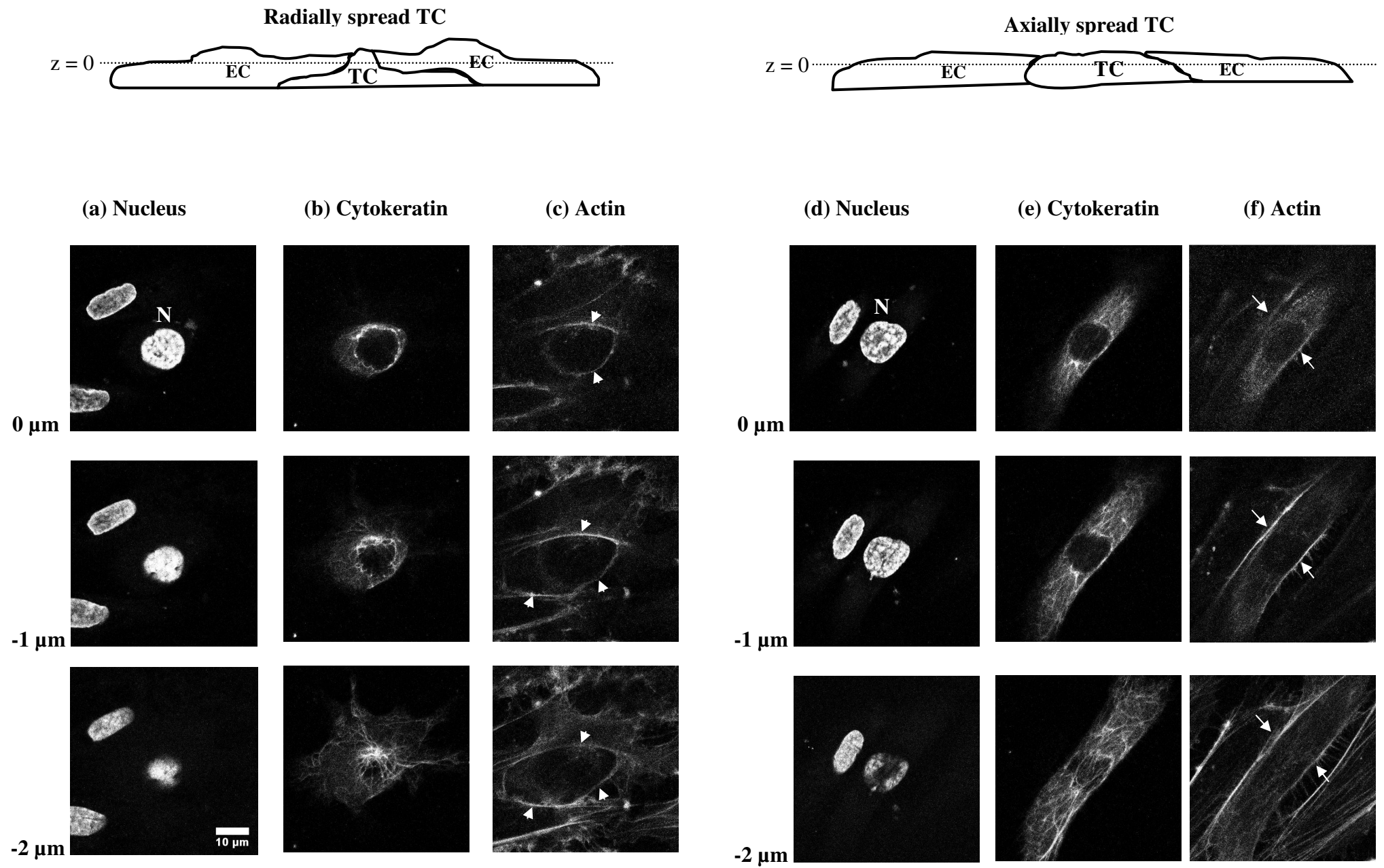


Fig.8